Progress In Electromagnetics Research Letters, Vol. 8, 9–17, 2009

DESIGN OF HIGH ORDER SUSPENDED STRIPLINE BANDPASS FILTER WITH MINIATURIZATION

M. Chen

Department of Industrial Engineering and Managenment
Chaoyang University of Technology
168, Jifong E. Road, Wufong, Taichung County 41349, Taiwan

C.-Y. Jiang

Graduate Institute of Communications Engineering
National Changhua University of Education
#1, Jin-De Road, Changhua City 50007, Taiwan

W.-Q. Xu

Universal Microwave Technology, Inc.
#1, Gongjian Road, Cidu District, Keelung City 20647, Taiwan

M.-H. Ho

Department of Electronic Engineering and Graduate Institute of Communications Engineering
National Changhua University of Education
#1, Jin-De Road, Changhua City 50007, Taiwan

Abstract—A quasi-lumped design of a suspended stripline (SSL) bandpass filter (BPF) exhibiting high signal selectivity is proposed. In the circuit, transmission zeros were implanted to enhance the stopband signal rejection. A sample BPF having an operation band of 6.77–7.33 GHz was fabricated and measured for performance verification of the proposed design.

Corresponding author: M.-H. Ho (ho@cc.ncue.edu.tw).

1. INTRODUCTION

In modern communication systems, filtering circuits mostly existing at the front end of a transceiver play import roles since they may significantly affect the system performance. In particular, in microwave and millimeter-wave system, front-end filters require characteristics of low insertion losses, high signal selectivity, steep band edge roll-off, high stopband rejection, and sometimes the size efficiency. Microstrips that have been widely used in building various kinds of filters exhibit insertion losses proportional to the operation frequency. The partial, yet strong, confinement electromagnetic fields in the dielectric also lead a microstrip to have high frequency dispersion and excessive losses.

The SSL structure was firstly proposed by Rooney and Underkofler in 1978 [1]. Recently, many applications in SSL filters and diplexers have been reported [2–5]. Compared with microstrips and coplanar waveguides, the SSL's dense air field distribution and low current density in the metal strip grant itself the advantages of low losses, low temperature sensitivity, low frequency dispersion, large bandwidth and suitability for high frequency operation. Moreover, its metal enclosure configuration can benefit the structure with high radiation immunity, and its surrounding ground can ease the shunt and series connections of lumped components. In this paper, we propose a 6th order BPF of the SSL structure. The concepts of quasi lumped element circuit given in [2, 6–8] are used to analyze the filter performance. Effort has been exerted on the circuit design to reduce the filter dimensions. The passband center frequency of a sample filter is set to 7 GHz, which can certainly be shifted to other frequencies, if desired, by using the same design procedure. The commercial electromagnetic software package, HFSS ver. 8.5, is used to verify the circuit design at the early stage. An experiment is subsequently conducted to validate the circuit performance. A good agreement is observed between the simulated and measured data.

2. FILTER DESIGN

The BPF of the SSL structure originates from a similar CPW filter design in [9]. The filter structure and its equivalent lumped-element circuit model are shown in Figs. 1(a) and 1(b), respectively. It is built on an RT/Duroid 5880 substrate with a thickness 0.254 mm, dielectric constant 2.2, and loss tangent 0.0009. The metal enclosure of the SSL is formed by a rectangular waveguide. The substrate is suspended horizontally in the middle of the metal shield with 2-mm thickness air zones above and below the substrate. The channel width of the

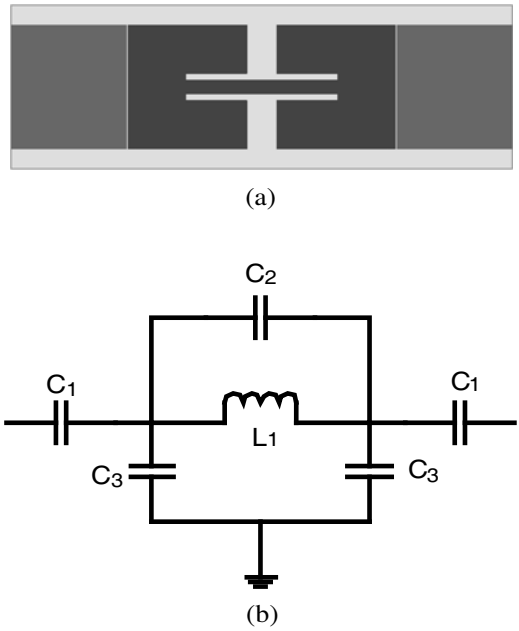

Figure 1. (a) The prototype SSL BPF structure and (b) the equivalent lumped element circuit model.

metal shield is 5 mm. The resonator in Fig. 1(a) (the part in dark color) is in a form of two connected hairpins. In the lumped-element circuit model, the narrow connection strip which confines the current on itself can be emulated by the series inductor, L_1. Also the open ends that face each other in the middle of the resonator accumulate charges of opposite polarizations, which is equivalent to the series capacitor, C_2. The couplings between upper/lower edges of the resonator and the bilateral ground are represented by the capacitors, C_3's. The I/O strips on the right and left sides of Fig. 1(a) (in shadow color) are laid on the bottom of the substrate, and their ends slightly overlap with the middle resonator. The capacitors, C_1's, denote the couplings between the I/O strips and the resonator. The resonance frequency (denoted by f_0) of the circuit is dominated by the relation

$$f_0 = \frac{1}{2\pi\sqrt{L_1(C_0 + C_2)}}. \tag{1}$$

where $C_0 = (C_1 + C_2)/2$.

The series block formed by parallel connection of L_1 and C_2, while in resonance it creates an open circuit in the middle of the

circuit, results in a transmission zero. The frequency of the zero, f_z, is dominated by

$$f_z = \frac{1}{2\pi\sqrt{L_1 C_2}}. \tag{2}$$

This prototype circuit belongs to the first-order circuit category which does not exhibit steep band edge roll-off. The second-order circuit is developed from modifying the prototype filter. It is achieved by shorting the middle of the narrow connection strip to the upper and lower grounds (seen from the top-view perspective, with the axis of the SSL oriented in the horizontal direction). This is performed by adding to the narrow connection strip, in the middle position, two vertical narrow strips for reaching the upper/lower grounds. To simplify the manufacturing complexity, the I/O strips are built on the same side, and an end coupling is used instead of the overlapped coupling in the second-order circuit design. The coupling gap is 0.1 mm. The width of the I/O strips is 3.8 mm, resulting in a 50 Ω characteristic impedance. The same width is adopted for the resonator, leading the I/O ports and the resonator to have a gap of 0.6 mm away from the upper and lower grounds.

Shown in Fig. 2 is the second-order BPF structure and its equivalent circuit model with all the element values given in the figure. The added vertical shorting strips correspond to the shunt inductor, L_2, which divides the series inductor L_1 of Fig. 1(b) into two identical inductors. The vertical strips block the coupling of the resonator's two open ends. Hence, the original capacitor C_2 in Fig. 1(b) converts to two capacitors C_2's in Fig. 2(b), which represent the couplings between the open ends and the vertical strips. Although they are blocked by the vertical strips, a very weak coupling, represented by a small-valued capacitor C_4, still exists between the two hairpins. In Fig. 3 we show the simulated frequency responses for the filter in Fig. 2 obtained from the circuit model and HFSS. It is evident that the second order BPF has two S_{11} dips in the passband region. A 3-dB passband of 6.67 to 7.62 GHz is obtained with a minimum insertion loss of 0.27 dB. Two transmission zeros located at 16.08 and 21.07 GHz are created in the stopband region. The extra zero is mainly caused by the added shunt inductor L_2 together with the shunt capacitors C_3's. Also clear is that the HFSS simulation confirms the validity of the proposed circuit model. Compared with the filter structure of Fig. 1, the modified filter in Fig. 2 using two $\lambda/4$ resonators (the one in Fig. 1 is a $\lambda/2$ resonator) occupies about the same circuit area, but doubles the circuit order. Hence, this size-reduction design is much more suitable for higher order filter applications.

In Fig. 4, we present the structure of a sample 6th order BPF

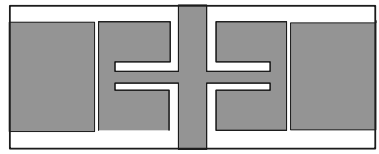

(a)

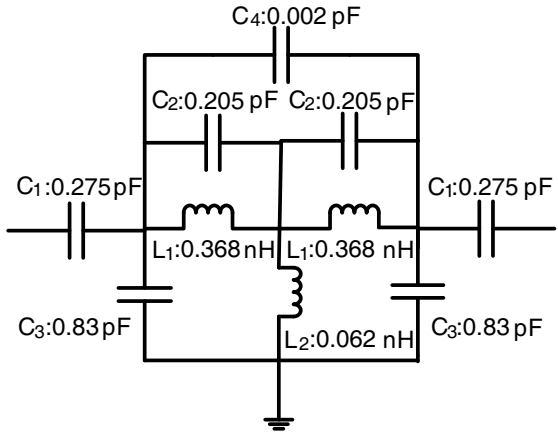

(b)

Figure 2. (a) The second-order BPF structure and (b) its equivalent circuit model.

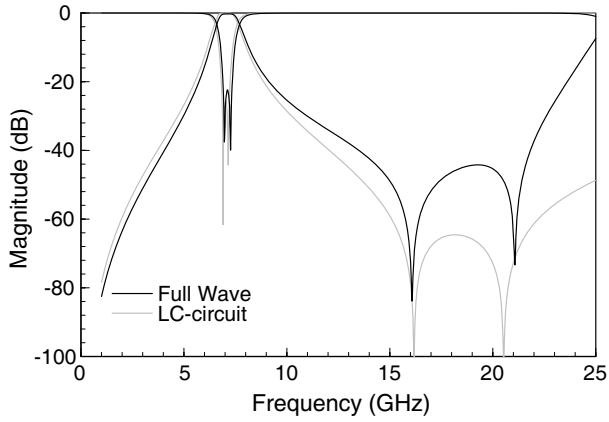

Figure 3. The simulated frequency responses from circuit model and HFSS.

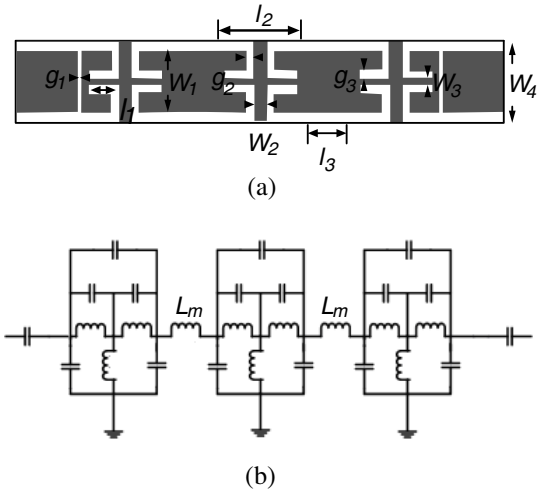

Figure 4. (a) The sample 6th-order BFP structure and (b) the equivalent lumped element circuit model.

and its equivalent lumped-element circuit model. The circuit is built by cascading three second-order filters of Fig. 2(a). The coupling structure between the two cascading circuit blocks is replaced by a section of short strip with the same width of 3.8 mm. This replacement is expected to eliminate the signal reflection caused by the coupling capacitance and reduce the insertion losses. This short connection strip is equivalent to a series inductor (denoted by L_m in Fig. 4(b)) in the lumped-element circuit model. Hence, instead of the electric coupling used in Fig. 1(a), the magnetic coupling is applied to the sample filter's inner block cascading. The input and output stages still use the capacitive coupling. The dimensions listed in Fig. 4(a) are $g_1 = 0.1$, $g_2 = 0.3$, $g_3 = 0.3$, $l_1 = 2.2$, $l_2 = 6.6$, $l_3 = 3.47$, $W_1 = 3.8$, $W_2 = 1$, $W_3 = 0.4$ and $W_4 = 5$, all in mm. The value of the equivalent coupling inductor is $L_m = 0.022$ nH which accounts for the connection strip with length l_3 in Fig. 4(a). The circuit only occupies an area of 5×26.74 mm^2 without including the I/O strips. The measured and simulated frequency responses are shown in Fig. 5. The calculated transmission zeros are 15.35 and 20.3 GHz which are slightly different from those in Fig. 3. The S_{21} dips at transmission zeros are too deep to be observed in the measurement; this might be owing to the insufficient dynamic range of the measurement equipment for $|S_{21}|$ below -60 dB, below which the detected signals are overwhelmed by the noise floor. The obtained circuit parameters are listed in Table 1.

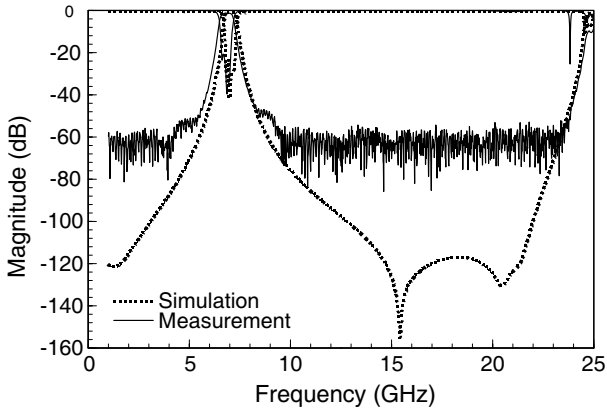

Figure 5. The measured and simulated frequency responses for BPF of Fig. 4(a).

The second harmonic of the $\lambda/4$ resonator for this filter is around 25 GHz which corresponds to the three quarter-wavelength resonance. The stopband bandwidth is about 17.3 GHz (247.6%) under the 20 dB signal rejection. Even though limited by the equipment's available dynamic range, the measured stopband signal rejection levels are still larger than 60 dB.

Table 1. The circuit parameters obtained from Fig. 5.

	measurement	simulation
Central frequency	6.91 GHz	7.02 GHz
Passband Range	$6.55 \sim 7.15$ GHz	$6.69 \sim 7.36$ GHz
Minimum Insertion loss	1.41 dB @ 6.91 GHz	0.75 dB @ 7.02 GHz

3. CONCLUSION

A high-order design of an SSL BPF is presented based on a size reduced second-order SSL BPF design. The filter and its lower-order counterparts were designed and optimized, by using a full-wave electromagnetic simulator, to operate around 7 GHz. With only little effort, such circuit structure is capable of shifting its center frequency to other desirable frequencies to support, e.g., WLAN and ISM bands. The behaviors of these filters were also simulated by employing the

equivalent lumped-element circuit models derived from their circuit layouts. Simulation and measurement were found to be in good agreement. Most attractive of all, the designed higher order SSL filter has achieved about a 247.6% (17.3 GHz) stopband fractional bandwidth (FBW) under a 20 dB out-of-band rejection. The measured passband's minimum insertion loss is around 1.41 dB at 6.91 GHz with an FBW of 8.7%. The insertion losses are considered very low for a 6th-order filter circuit. The insertion losses mostly attribute to the conductor losses of the vertical strips connecting to the upper and lower grounds since the current is dense there. The stopband BW is limited by the second resonance (a three quarter-wavelength resonance) of the quarter-wavelength resonator.

The performance of the proposed SSL filter is superior to its originated CPW filter design in [9] which has a minimum insertion loss of 2.52 dB at 2.48 GHz, a stopband FBW of 201%, and the stopband signal rejection levels between 20–40 dB. The proposed filter, even being a circuit of 6th-order, still possesses a smaller minimum insertion loss at a much higher frequency. And it has a wider stopband BW (FBW) with all the signal rejection levels, in the stopband region, over 60 dB. Moreover, the continuous cascading between the circuit blocks eliminates the signal reflection and renders this BPF a suitable circuit in a much higher order filter design. It is believed that this compact design of SSL BPF with such a wide stopband is suitable for many modern wireless communication systems.

ACKNOWLEDGMENT

The authors wish to acknowledge the valuable comments provided by Prof. C.-I. G. Hsu of National Yunlin University of Technology and Prof. C.-H. Lee of National Changhua University of Education. The support of National Science Committee of R.O.C. under the grant No. NSC 97-2221-E-018-004-MY2 is also acknowledged.

REFERENCES

1. Rooney, J. P. and L. M. Underkofler, "Printed circuit integration of microwave filters," *Microwave J.*, Vol. 21, No. 9, 68–73, Sep. 1978.
2. Menzel, W. and A. Balalem, "Quasi-lumped suspended stripline filters and diplexers," *IEEE Trans. Microwave Theory Tech.*, Vol. 53, No. 10, 3230–3237, Oct. 2005.
3. Menzel, W., M. S. R. Tito, and L. Zhu, "Low-loss ultra-wideband

(UWB) filters using suspended stripline," *Proc. Asia-Pacific Microwave Conf.*, Vol. 4, 2148–2151, Dec. 2005.

4. Menzel, W., "A novel miniature suspended stripline filter," *European Microwave Conf. Dig.*, 1047–1050, Munich, Oct. 2003.
5. Lin, L.-J., M.-H. Ho, and W.-Q. Xu, "Design of compact suspended stripline bandpass filters with wide stopband," *Microwave and Optical Technology Lett.*, Vol. 50, No. 4, 865–868, Apr. 2008.
6. Xu, W.-Q., M.-H. Ho, and C.-I. G. Hsu, "Quasi-lumped design of UMTS diplexer using combined CPW and microstrip," *Microwave and Optical Technology Lett.*, Vol. 51, No. 1, 150–152, Jan. 2009.
7. Nosrati, M., T. Faraji, and Z. Atlasbaf, "A compact composite broad top-band ellipticfunction low-pass filter for ultra wideband applications using interdigital capacitors," *Progress In Electromagnetics Research Letters*, Vol. 7, 87–95, 2009.
8. Wu, M.-S., Y.-Z. Chueh, J.-C. Yeh, and S.-G. Mao, "Synthesis of triple-band and quad-band bandpass filters using lumped-element coplanar waveguide resonators," *Progress In Electromagnetics Research B*, Vol. 13, 433–451, 2009.
9. Lin, L.-J., M.-H. Ho, and W.-Q. Xu, "Design of compact CPW bandpass filters with wide stopband," *Microwave and Optical Technology Lett.*, Vol. 49, No. 4, 973–976, Apr. 2007.